Shape Control of Composite Plates and Shells with Embedded Actuators. II. Desired Shape Specified

DAVID B. KOCONIS, LÁSZLÓ P. KOLLÁR*
AND GEORGE S. SPRINGER
Department of Aeronautics and Astronautics
Stanford University
Stanford, CA 94305

(Received March 9, 1993)
(Revised August 9, 1993)

ABSTRACT: The changes in shapes of fiber-reinforced composite beams, plates and shells affected by embedded piezoelectric actuators were investigated. An analytical method was developed to determine the voltages needed to achieve a specified desired shape. The method is formulated on the basis of mathematical models using two-dimensional, linear, shallow shell theory including transverse shear effects which are important in the case of sandwich construction. The solution technique is a minimization of an error function which is a measure of the difference between the deformed shape caused by the application of voltages and the desired shape. A computationally efficient, user-friendly computer code was written which is suitable for performing the numerical calculations. The code, designated as SHAPE2, gives the voltages needed to achieve specified changes in shape. To validate the method and the computer code, results generated by the code were compared to existing analytical and experimental results. The predictions provided by the SHAPE2 code were in excellent agreement with the results of the other analyses and data.

1. INTRODUCTION

DURING THE COURSE of this investigation two analytical models were developed which are applicable to two different types of problems (Figure 1 in Reference [1]). The first model is presented in Reference [1], and is for calculating the changes in shapes of beams, plates and shells when the voltages applied to the piezoelectric actuators are given. The second model is presented in this paper, and is for determining the voltages needed to achieve a prescribed shape.

A brief summary of previous work as it applies to piezoelectric actuator induced shape control appears in a companion paper [1]. All of the methods pre-

*On leave from the Technical University of Budapest, Hungary.

0021-9983/94/05 459-24 $6.00/0

sented provide, for each specific problem, the change in shape under a given applied voltage. None of them can handle the "inverse problem" in which the voltage needed to achieve a specified shape change is to be determined.

2. PROBLEM STATEMENT

Here we consider the problem in which the original shape and actuator configuration of a structure are known and a desired shape is specified (Problem 2 in Figure 1 in Reference [1]). It is desired to find the set of voltages needed which must be applied to the piezoelectric actuators to achieve the prescribed shape. This type of information is needed in the operation of piezoelectric actuator systems, namely in determining the magnitudes of voltages required for efficient shape control.

We consider six different structural elements: (1) straight beam, (2) curved beam (3) rectangular plate, (4) circular plate, (5) rectangular shell, and (6) circular shell (Figure 2 in Reference [1]). The element considered may be supported along any of its edges or at one or more locations on the top and bottom surfaces. The supports may be "built-in," "fixed" or "hinged," as illustrated in Figure 3 in Reference [1]. Each of these elements may be a "solid" laminate, or may be of sandwich construction consisting of an orthotropic core covered by two face sheets. The solid laminate or the face sheets may be made of a single material or of different materials bonded together. The layers (plies) may be arranged in any sequence, and the thicknesses of the layers may be different. Each layer may be isotropic or orthotropic, the latter including continuous unidirectional fiber-reinforced composites. Perfect bonding is assumed to exist between the layers themselves and between the face sheets and the core.

Piezoelectric actuators may be mounted on the surfaces or embedded inside the material (Figure 4 in Reference [1]). These actuators may be isotropic or orthotropic and may either be continuous extending over the entire area of the element, or they may be applied in discrete patches. The continuous actuators may be located on the surface or at one or more locations inside the material. Rectangular or circular patches of arbitrary thickness can only be on the top or bottom surfaces.

Upon the application of a voltage to each piezoelectric actuator, the actuator exerts a force on the material, changing the shape of the structure. The objective of this investigation was to determine the applied voltage required to achieve a prescribed change in shape.

The shape of the element is described via a suitably chosen "reference" surface. The shape of this reference surface is defined by a single z_o-coordinate of every point on the surface, as illustrated in Figure 5 in Reference [1]. Note that the z_o-coordinate is perpendicular to an x-y plane. The shape must be such that the z_o-coordinate of every point can be specified by a polynomial function in x and y

$$z_o = \sum a_i x^{n_i} y^{m_i} \tag{1}$$

where a_i are constants and m_i and n_i are integers equal to or greater than zero.

3. METHOD OF ANALYSIS

In this section we consider the problem in which the element construction (face sheet lay-up, core thickness, and number and location of piezoelectric actuators) is given and remains constant. The element is rigidly supported at one or more points or is free-standing (not supported at all). The original shape and the desired new shape of the structural element are specified. It is required to find the voltage which must be applied to each actuator to achieve the desired new shape. In general, it is desired to apply as small a voltage as possible. Hence, the goal is to find the smallest amount of voltage which results in the required shape.

The analysis is based on small deformation theory. Therefore, the specified desired shape must be within the region of "small deformation" from the original shape. Furthermore, the analysis uses the shape change of a reference surface (Section 2). The desired shape is generally prescribed by the shape of the "top" or "bottom" surface of the element. In this case, within the approximations used in this study, the shapes of either the "top" or the "bottom" surface of the element can be taken as the reference surface [2].

The analysis utilizes an x, y, and z Cartesian coordinate system with its origin at a suitable reference point on the reference surface of the element (Figure 1). This reference point is located either at a fixed support or, in the case of a free-standing element, at an arbitrary point. At this reference point the linear and angular displacements of the desired new shape and of the original shape are forced to match.

3.1 Error Function Λ

As a starting point we assume that a given set of voltages is applied which results in a change in the shape of the element (dashed line in Figure 2). We introduce an error function which includes the difference between the intermediate

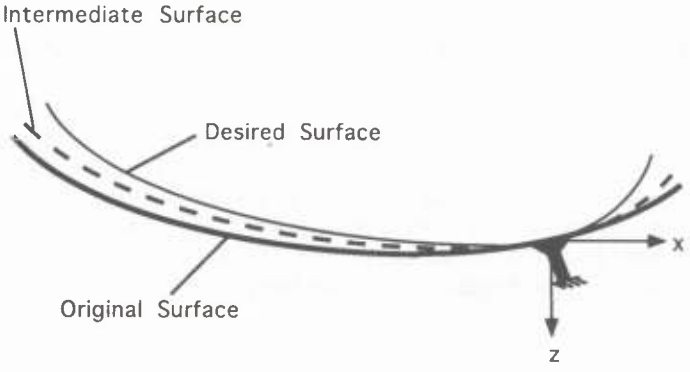

Figure 1. *Original surface, intermediate surface, and desired surface in the* x-z *plane.*

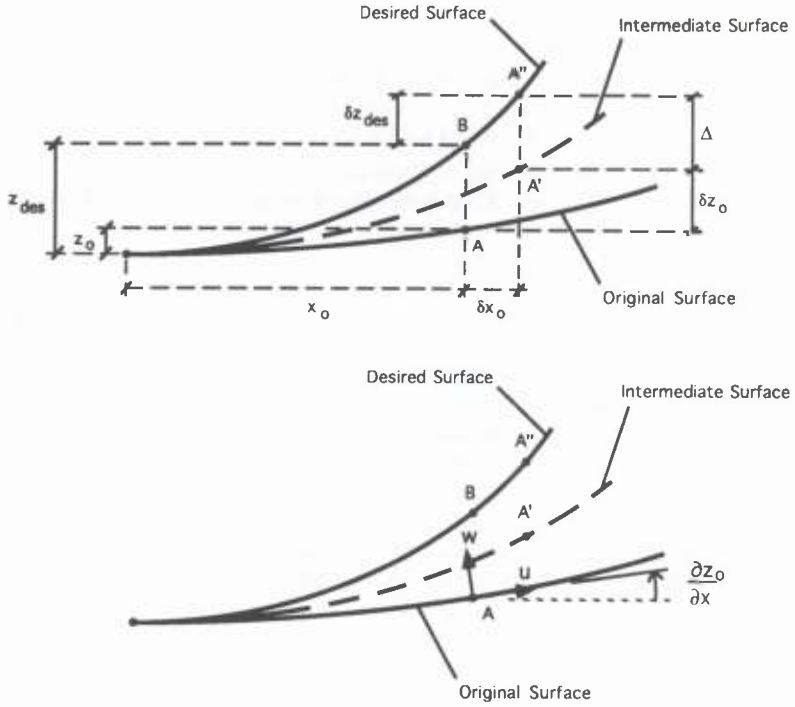

Figure 2. *Illustration of the difference between the intermediate surface and the desired surface in the x-z plane.*

shape and the desired one and the total amount of voltage employed. The error function has the form

$$\Lambda = \Gamma\Lambda_1 + \Lambda_2 \tag{2}$$

where Λ_1 is proportional to the amount of voltage applied, Λ_2 is proportional to the distance between the reference surface of the desired shape and the intermediate reference surface, and Γ is a weight factor. Λ has units of length^2, Λ_1: voltage^2, Λ_2: length^2, and Γ: length^2/voltage^2. Generally we wish to affect the required shape change using the smallest amount of applied voltage. The objective then is to make the error function Λ as small as possible such that the desired surface and the intermediate surface are nearly identical (i.e., $\Lambda_2 \rightarrow 0$), and a minimum amount of applied voltage is used (i.e., $\Lambda_1 \rightarrow 0$).

In Equation (2), the function Λ_1 has the form

$$\Lambda_1 = \sum_{i=1}^{n_{el}} A_i e_i^2 \tag{3}$$

where e_i is the voltage applied at the ith electric layer or patch of area A_i, and n_{el} is the total number of electric layers or patches. The factor Γ signifies the importance that is paid to the magnitude of the applied voltages. If the magnitude of the applied voltages is of no concern (and any amount of voltage can be applied), Γ is set to zero. If, on the other hand, as small amount of voltage as possible is to be used, Γ is set to a high value (say, $\Gamma = 1 \times 10^{-10}$ in^2/V^2). The function Λ_2 has the form

$$\Lambda_2 = \iint_{\Omega} \Delta^2 dxdy \tag{4}$$

where Ω represents the element domain (Figure 6 in Reference [1]), and Δ represents the difference between the z-coordinate of a point on the reference surface of the desired shape and the z-coordinate of a corresponding point on the intermediate reference surface.

The distance Δ is defined as (Figure 2)

$$\Delta = (z_o + \delta z_o) - (z_{des} + \delta z_{des}) \tag{5}$$

In order to understand each of the terms in Equation (5), consider a point A on the original reference surface at (x_o, y_o) (Figure 2). z_o is the z-coordinate of the point A on the original reference surface. δz_o is the difference between the z-coordinate of point A on the original reference surface, and the z-coordinate of the corresponding point A′ on the intermediate reference surface. δz_o may be expressed as (Figure 2)

$$\delta z_o = \left(u \frac{\partial z_o}{\partial x} + v \frac{\partial z_o}{\partial y} + w \right)_A \tag{6}$$

where u, v, and w are the displacements of A. u is the displacement tangential to the reference surface in the off-axis x-z plane, v is the displacement tangential to the reference surface in the off-axis y-z plane, and w is the deflection normal to the reference surface (Figure 6 in Reference [1]). z_{des} is the z-coordinate of point B on the desired reference surface at (x_o, y_o). The point on the desired reference surface corresponding to point A′ on the intermediate reference surface is point A″ located at $(x_o + \delta x_o, y_o + \delta y_o)$. δz_{des} is the difference between the z-coordinates of points A″ and B. It can be approximated by the first two terms of a Taylor series expansion

$$\delta z_{des} = \left(\frac{\partial z_{des}}{\partial x} \right)_B \delta x_o + \left(\frac{\partial z_{des}}{\partial y} \right)_B \delta y_o \tag{7}$$

The distances δx_o and δy_o are the changes in the x- and y-coordinates between points A″ and B (Figure 2)

$$\delta x_o = \left(u - w \frac{\partial z_o}{\partial x} \right)_A \qquad \delta y_o = \left(v - w \frac{\partial z_o}{\partial y} \right)_A \tag{8}$$

For convenience, the following three parameters, which depend on the geometries of the original and desired surfaces, are introduced

$$\eta_1 = 1 + \left(\frac{\partial z_{des}}{\partial x}\right)_B \left(\frac{\partial z_o}{\partial x}\right)_A + \left(\frac{\partial z_{des}}{\partial y}\right)_B \left(\frac{\partial z_o}{\partial y}\right)_A$$

$$\eta_2 = \left(\frac{\partial z_o}{\partial x}\right)_A - \left(\frac{\partial z_{des}}{\partial x}\right)_B \tag{9}$$

$$\eta_3 = \left(\frac{\partial z_o}{\partial y}\right)_A - \left(\frac{\partial z_{des}}{\partial y}\right)_B$$

With the use of these parameters, Equations (4) through (8) can be rearranged to yield the following expression for Λ_2

$$\Lambda_2 = \int\int_{\Omega} [(z_o - z_{des}) + \eta_1 w + \eta_2 u + \eta_3 v]^2 dxdy \tag{10}$$

Until this point, the analysis presented applies to piezoelectric materials which behave linearly or nonlinearly (Equations (11) and (16) in Reference [1]) with respect to the applied voltages. In the analysis that follows, only piezoelectric materials with a linear strain-voltage relationship (Equation (11) in Reference [1]) are considered. For these materials, the voltages may be factored out of the displacements u, v, and w in Equation (10) by introducing the matrices $\bar{\mathbf{u}}$, $\bar{\mathbf{v}}$, and $\bar{\mathbf{w}}$. The components of the $\bar{\mathbf{u}}$, $\bar{\mathbf{v}}$, and $\bar{\mathbf{w}}$ matrices are defined as follows. The displacements u, v, and w are given by (see Table 3 in Reference [1]).

$$u = \mathbf{f} \cdot \mathbf{u} \qquad v = \mathbf{g} \cdot \mathbf{v} \qquad w = \mathbf{h} \cdot \mathbf{w} \tag{11}$$

where $\mathbf{f}$, $\mathbf{g}$, and $\mathbf{h}$ are the vectors of the trial functions for the displacements u, v, and w, respectively, and $\mathbf{u}$, $\mathbf{v}$, and $\mathbf{w}$ are the vectors of corresponding coefficients. If we now apply a unit voltage at the first piezoelectric actuator (with no voltage at any other actuator) we obtain a set of u, v, and w displacements. The components of the $\mathbf{u}$, $\mathbf{v}$, and $\mathbf{w}$ vectors thus obtained form the first column of the $\bar{\mathbf{u}}$, $\bar{\mathbf{v}}$, and $\bar{\mathbf{w}}$ matrices. The application of a voltage at the second piezoelectric actuator (with no voltage at any other actuator) results in different u, v, and w displacements. The components of the $\mathbf{u}$, $\mathbf{v}$, and $\mathbf{w}$ vectors thus obtained form the second column of the $\bar{\mathbf{u}}$, $\bar{\mathbf{v}}$, and $\bar{\mathbf{w}}$ matrices. The subsequent columns are formed in a similar manner. Numerical values of the components of the $\bar{\mathbf{u}}$, $\bar{\mathbf{v}}$, and $\bar{\mathbf{w}}$ matrices must be obtained by the analysis presented in Reference [1]. Note that the desired shape is limited to the linear combination of the possible deformed shapes resulting from the trial functions. The analysis then minimizes Λ and gives the "best" desired shape within this constraint.

Using the aforementioned notation, the error function Λ_2 is written as

$$\Lambda_2 = \iint_{\Omega} [(z_o - z_{des}) + (\eta_1 \mathbf{h}\bar{\mathbf{w}} + \eta_2 \mathbf{f}\bar{\mathbf{u}} + \eta_3 \mathbf{g}\bar{\mathbf{v}})\mathbf{e}]^2 dxdy \tag{12}$$

where $\mathbf{e}$ is the vector containing the n_{el} voltages e_i at every layer or patch. Note that in the form written above, Λ_2 is expressed as a function of $\mathbf{e}$ and not Δ as in Equation (4).

3.2 Method of Solution 1

Inspection of Equations (3) and (12) reveals that both Λ_1 and Λ_2, and hence Λ, can be expressed in terms of the applied voltages. Therefore, the objective to have as small an error function as possible is achieved by minimizing Λ with respect to the applied voltages $\mathbf{e}$. This objective is accomplished when the following condition is met

$$\frac{\partial \Lambda}{\partial \mathbf{e}} = 0 \tag{13}$$

By substituting Equations (3) and (12) into Equation (13) and by performing the differentiation we obtain

$$\mathbf{R}_{ei}\mathbf{e} - \mathbf{R}_{s1} = \mathbf{0} \tag{14}$$

where $\mathbf{R}_{ei}$ and $\mathbf{R}_{s1}$ are defined in Table 1.

The unknown voltages required to achieve the desired shape are determined by solving Equation (14) for $\mathbf{e}$. The result is

$$\mathbf{e} = \mathbf{R}_{ei}^{-1}\mathbf{R}_{s1} \tag{15}$$

The foregoing analysis is applicable when there are no temperature induced changes in the shape and when rigid body motions are not permitted. The effects of temperature are included in Reference [2].

The analysis pertaining to elements which are supported in such a way that rigid body motion is feasible is presented below. This analysis is not only useful when rigid body motion is feasible but also when the supports are fixed, and rigid body motion is impossible. In this situation we have two choices, (1) to apply the analysis presented above or (2) to assume that a rigid body motion is permitted, perform the calculations as described in the next section (Section 3.3) then set the resulting rigid body motion to zero. In most cases the latter approach will result in a better approximation to the desired shape than the first approach.

3.3 Rigid Body Motions

In the foregoing analysis, the element was rigidly fixed at least at one point. In this section we consider the case when the element is attached to one or more

Table 1. Definitions of $\mathbf{R}_{ei}$ and $\mathbf{R}_{s1}$.

Term	Definition
$\mathbf{R}_{ei}$	$\bar{\mathbf{w}}^T \iint_\Omega \mathbf{h}^T \mathbf{h} \eta_1^2 dxdy \bar{\mathbf{w}}$
	$+ 2\bar{\mathbf{u}}^T \iint_\Omega \mathbf{f}^T \mathbf{h} \eta_1 \eta_2 dxdy \bar{\mathbf{w}}$
	$+ 2\bar{\mathbf{v}}^T \iint_\Omega \mathbf{g}^T \mathbf{h} \eta_1 \eta_3 dxdy \bar{\mathbf{w}}$
	$+ \bar{\mathbf{u}}^T \iint_\Omega \mathbf{f}^T \mathbf{f} \eta_2^2 dxdy \bar{\mathbf{u}}$
	$+ \bar{\mathbf{v}}^T \iint_\Omega \mathbf{g}^T \mathbf{g} \eta_3^2 dxdy \bar{\mathbf{v}}$
	$+ 2\bar{\mathbf{u}}^T \iint_\Omega \mathbf{f}^T \mathbf{g} \eta_2 \eta_3 dxdy \bar{\mathbf{v}} + \Gamma \hat{\mathbf{A}}$
$\mathbf{R}_{s1}$	$\bar{\mathbf{w}}^T \iint_\Omega \mathbf{h}^T (z_{des} - z_o) \eta_1 dxdy$
	$+ \bar{\mathbf{u}}^T \iint_\Omega \mathbf{f}^T (z_{des} - z_o) \eta_2 dxdy$
	$+ \bar{\mathbf{v}}^T \iint_\Omega \mathbf{g}^T (z_{des} - z_o) \eta_3 dxdy$

where $\hat{\mathbf{A}}$ is a diagonal matrix containing the areas A_i of the electric layers or patches

$$\hat{\mathbf{A}} = \begin{bmatrix} A_1 & 0 & \cdots & 0 \\ 0 & A_2 & \cdots & 0 \\ \vdots & \vdots & \ddots & \vdots \\ 0 & 0 & \cdots & A_{nel} \end{bmatrix}$$

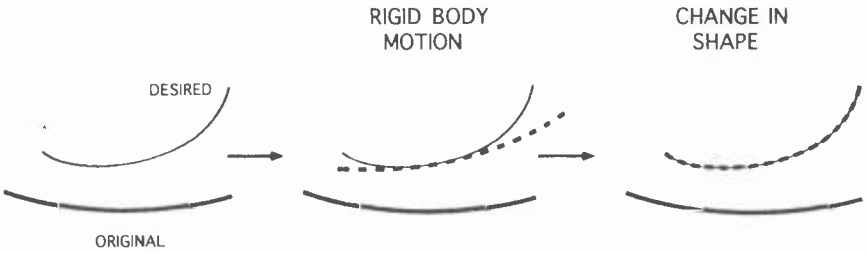

Figure 3. *Illustration of the steps taken to achieve a desired shape. First the original shape is translated and/or rotated. Then voltages are applied to cause a shape change.*

supports which may impart a force to the element. This force may result in a rigid body motion (translation and rotation) but not in a change in shape. Under this circumstance the new location and shape of the element can be reached by a combination of rigid body motion and change in shape (Figure 3). The rigid body motion is described by the linear and angular displacements of an arbitrarily chosen reference point R on the reference surface (C_x, C_y, C_z, θ_x, θ_y, and θ_z in Figure 4). In the analysis we strive to find the magnitudes of each of these six

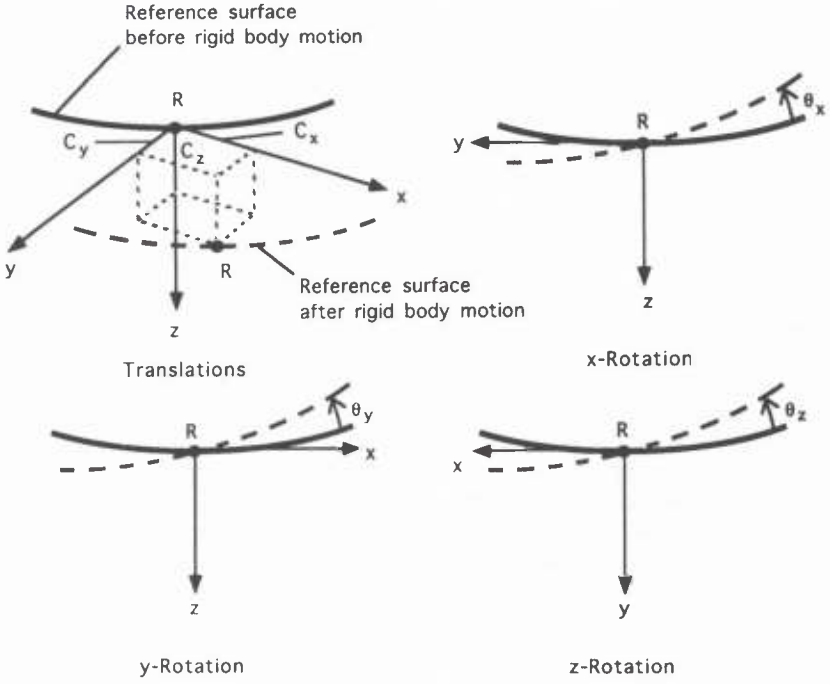

Figure 4. *Linear and angular displacements of a reference point.*

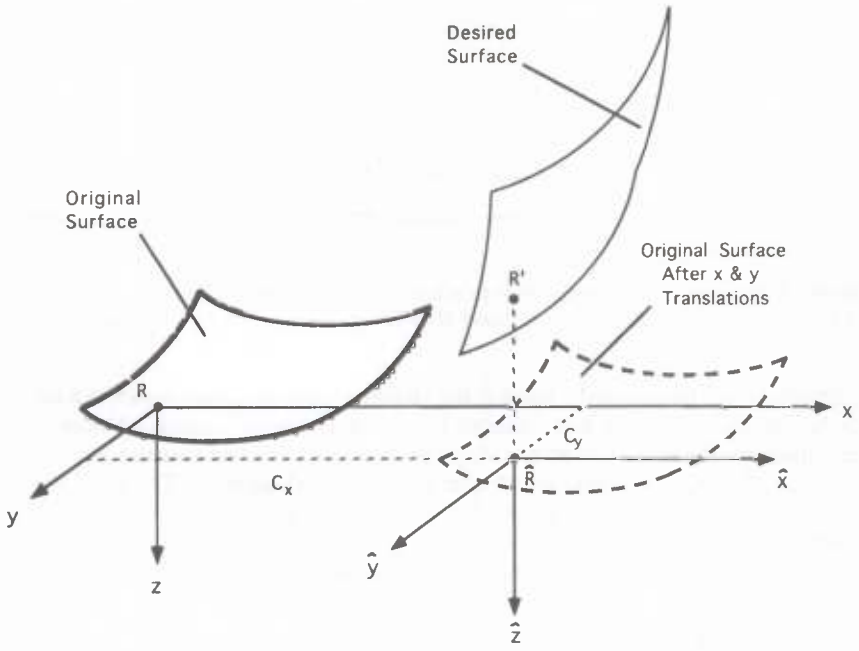

Figure 5. *Illustration of the reference point on the original surface and corresponding point on the desired surface.*

rigid body displacements as well as the minimum amount of voltage which must be applied to each piezoelectric actuator to achieve the desired location and shape of the element.

The analysis begins by choosing a reference point R on the original surface which is the origin of the x-y-z coordinate system (Figure 5). The position of the corresponding point on the desired surface is R′. Now we allow the original reference surface to undergo a rigid body translation in the x-y plane so that the reference point P. stays in the plane and moves to $\hat{R}$ (Figure 5). The magnitude of these translations are denoted, respectively, C_x and C_y. After this translation, R (which now coincides with $\hat{R}$) lies directly "underneath" R′, meaning that $\hat{R}$ and R′ are on the same line perpendicular to the x-y plane. The point $\hat{R}$ is the origin for a new $\hat{x}$-$\hat{y}$-$\hat{z}$ coordinate system where $\hat{x} = x - C_x$, $\hat{y} = y - C_y$, and $\hat{z} = z$. Now we assume that a given set of voltages is applied which results in a change of shape denoted as Intermediate Surface 1 (dashed line a–b in Figure 6). In addition, we now include a given set of rigid body z-translation and rotations about the $\hat{x}$-, $\hat{y}$-, and $\hat{z}$-axes, which results in a new location and orientation of the intermediate surface (Intermediate Surface 2; dashed line c–d). The error function Λ is again introduced; its form remains the same as in Equation (2)

$$\Lambda = \Gamma\Lambda_1 + \Lambda_2 \tag{16}$$

Λ_1 is given by Equation (3) and is unaffected by the rigid body motion since it only involves the magnitude of the voltages **e**. However, Λ_2 must be modified since the position of intermediate surface 2 includes the effects of the rigid body motion. The form of Λ_2 is the same as Equation (4) with Δ replaced by $\hat{\Delta}$.

$$\Lambda_2 = \iint_{\Omega} \hat{\Delta}^2 d\hat{x} d\hat{y} \tag{17}$$

The distance $\hat{\Delta}$ is defined as (Figure 7)

$$\hat{\Delta} = (\hat{z}_o + \delta\hat{z}_o + \delta_{o_{rb}}) - (\hat{z}_{des} + \delta\hat{z}_{des} + \delta\hat{z}_{des_{rb}}) \tag{18}$$

The terms in Equation (18) may be understood by considering a point $\hat{A}$ on the original surface located at $(\hat{x}_o, \hat{y}_o)$ (Figure 7). $\hat{z}_o$ is the $\hat{z}$-coordinate of point $\hat{A}$ on the original surface. $\delta\hat{z}_o$ is the difference between the $\hat{z}$-coordinate of point $\hat{A}$ on the original surface and the $\hat{z}$-coordinate of the corresponding point A′ on intermediate surface 1 (Figure 7). $\delta\hat{z}_o$ is obtained analogously to Equation (6)

$$\delta\hat{z}_o = \left(u \frac{\partial \hat{z}_o}{\partial \hat{x}} + v \frac{\partial z_o}{\partial \hat{y}} + w \right)_{\hat{A}} \tag{19}$$

$\delta\hat{z}_{o_{rb}}$ is the difference between the $\hat{z}$-coordinate of the point A′ on intermediate surface 1 and the corresponding point A‴ on intermediate surface 2. The form of $\delta\hat{z}_{o_{rb}}$ is discussed subsequently. $\hat{z}_{des}$ is the $\hat{z}$-coordinate of point B on the desired surface corresponding to point $\hat{A}$. The point on the desired surface corresponding to point A′ on intermediate surface 1 is point A″ located at

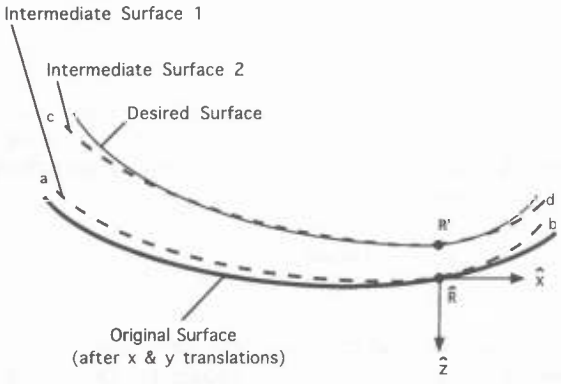

Figure 6. *Original surface, intermediate surface 1, intermediate surface 2, and the desired surface in the* x-z *plane.*

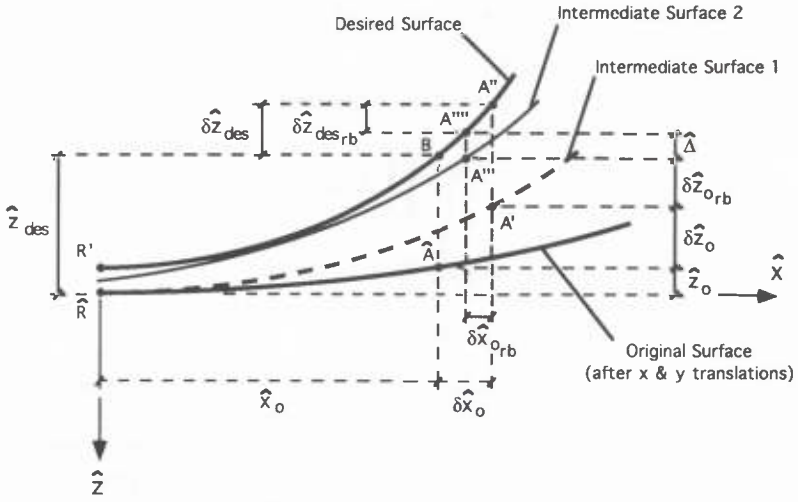

Figure 7. *Illustration of the difference between intermediate surface 1, intermediate surface 2, and the desired surface in the x-z plane.*

$(\hat{x}_o + \delta\hat{x}_o, \hat{y}_o + \delta\hat{y}_o)$. $\delta\hat{z}_{des}$ is the difference between the $\hat{z}$-coordinates of points A″ and B. $\delta\hat{z}_{des}$ is approximated analogously to Equation (7)

$$\delta\hat{z}_{des} = \left(\frac{\partial\hat{z}_{des}}{\partial\hat{x}}\right)_B \delta\hat{x}_o + \left(\frac{\partial\hat{z}_{des}}{\partial\hat{y}}\right)_B \delta\hat{y}_o \tag{20}$$

The distances $\delta\hat{x}_o$ and $\delta\hat{y}_o$ are the changes in the $\hat{x}$- and $\hat{y}$-coordinates between points A″ and B

$$\delta\hat{x}_o = \left(u - w\frac{\partial\hat{z}_o}{\partial\hat{x}}\right)_{\hat{A}} \qquad \delta\hat{y}_o = \left(v - w\frac{\partial\hat{z}_o}{\partial\hat{y}}\right)_{\hat{A}} \tag{21}$$

The point on the desired reference surface corresponding to point A‴ is point A⁗ located at $(\hat{x}_o + \delta\hat{x}_o + \delta\hat{x}_{o_{rb}}, \hat{y}_o + \delta\hat{y}_o + \delta\hat{y}_{o_{rb}})$. $\delta\hat{z}_{des_{rb}}$ is the difference between the points A⁗ and A″. As with $\delta\hat{z}_{des}$, it can be approximated by the first two terms of a Taylor series expansion

$$\delta\hat{z}_{des_{rb}} = \left(\frac{\partial\hat{z}_{des}}{\partial\hat{x}}\right)_B \delta\hat{x}_{o_{rb}} + \left(\frac{\partial\hat{z}_{des}}{\partial\hat{y}}\right)_B \delta\hat{y}_{o_{rb}} \tag{22}$$

The distances $\delta\hat{x}_{o_{rb}}$ and $\delta\hat{y}_{o_{rb}}$ are the changes in the $\hat{x}$- and $\hat{y}$-coordinates between points A⁗ and A″ and are discussed subsequently. The derivatives in Equation (22) should be evaluated at A″. However, we evaluate the derivatives at B. This approximation is reasonable because points A″ and B are close.

In order to explain the forms of $\delta\hat{x}_{o_{rb}}$, $\delta\hat{y}_{o_{rb}}$, and $\delta\hat{z}_{o_{rb}}$, we must examine the rigid body motions themselves. There are four possible rigid body motions remaining; one translation in the $\hat{z}$-coordinate direction and three rotations, one each about the coordinate axes $\hat{x}$, $\hat{y}$, and $\hat{z}$. Each one of these remaining rigid body motions has associated with it a set of resulting displacements $\delta\hat{x}_{o_{rb}}$, $\delta\hat{y}_{o_{rb}}$, and $\delta\hat{z}_{o_{rb}}$. These displacements can be written as

$$\delta\hat{x}_{o_{rb}} = \mathbf{x}_{rb}^T \mathbf{C}_{rb} \qquad \delta\hat{y}_{o_{rb}} = \mathbf{y}_{rb}^T \mathbf{C}_{rb} \qquad \delta\hat{z}_{o_{rb}} = \mathbf{z}_{rb}^T \mathbf{C}_{rb} \tag{23}$$

where $\mathbf{x}_{rb}$, $\mathbf{y}_{rb}$, and $\mathbf{z}_{rb}$ are vectors containing the $\hat{x}$, $\hat{y}$, and $\hat{z}$ displacements associated with each of the rigid body motions.

$$\mathbf{x}_{rb} = \begin{Bmatrix} 0 \\ 0 \\ \hat{z}_o \\ -\hat{y}_o \end{Bmatrix} \qquad \mathbf{y}_{rb} = \begin{Bmatrix} 0 \\ \hat{z}_o \\ 0 \\ \hat{x}_o \end{Bmatrix} \qquad \mathbf{z}_{rb} = \begin{Bmatrix} 1 \\ -\hat{y}_o \\ -\hat{x}_o \\ 0 \end{Bmatrix} \tag{24}$$

$\mathbf{C}_{rb}$ is the vector containing the as yet unknown magnitudes of each rigid body motion

$$\mathbf{C}_{rb} = \begin{Bmatrix} C_z \\ \theta_x \\ \theta_y \\ \theta_z \end{Bmatrix} \tag{25}$$

The equations in (23) are summarized in Table 2. In this table, small rotation angles are assumed so that $\sin\theta \approx \theta$ and $\cos\theta \approx 1$. The subscript o refers to the coordinates of point $\hat{A}$ in the $\hat{x}$-$\hat{y}$-$\hat{z}$ coordinate system on the original surface after the x and y translations. With the aforementioned procedure for including rigid body motions, four new unknown constants have been introduced into the problem via the vector $\mathbf{C}_{rb}$.

The above equations apply when the piezoelectric material behavior is either linear or nonlinear (Equations (11) and (16) in Reference [1]). We now restrict the analysis to piezoelectric materials for which the strain-voltage relationship is

Table 2. Displacements associated with the four remaining rigid body motions.

Motion	$\delta\hat{x}_{o_{rb}}$	$\delta\hat{y}_{o_{rb}}$	$\delta\hat{z}_{o_{rb}}$
z-Translation	0	0	C_z
Rotation about the $\hat{x}$-axis	0	$\hat{z}_o\theta_x$	$-\hat{y}_o\theta_x$
Rotation about the $\hat{y}$-axis	$\hat{z}_o\theta_y$	0	$-\hat{x}_o\theta_y$
Rotation about the $\hat{z}$-axis	$-y_o\theta_z$	$\hat{x}_o\theta_z$	0

linear. Then by using Equations (18) through (23) and the notation developed in Section 3.1, Equation (12) may be rewritten

$$\Lambda_2 = \int\int_{\Omega}\Bigg[(\hat{z}_o - \hat{z}_{des}) + (\eta_1 \mathbf{h}\bar{\mathbf{w}} + \eta_2 \mathbf{f}\bar{\mathbf{u}} + \eta_3 \mathbf{g}\bar{\mathbf{v}})\mathbf{e} + \left(\mathbf{z}_{rb}^T - \frac{\partial z_{des}}{\partial x}\mathbf{x}_{rb}^T - \frac{\partial z_{des}}{\partial y}\mathbf{y}_{rb}^T\right)\mathbf{C}_{rb}\Bigg]^2 d\hat{x}d\hat{y} \tag{26}$$

As before, Λ_2 does not depend explicitly on $\hat{\Delta}$, but does depend on $\mathbf{e}$ and $\mathbf{C}_{rb}$.

3.4 Method of Solution 2

The objective now is to minimize the total error function Λ with respect to the applied voltages $\mathbf{e}$ and the rigid body motion coefficients $\mathbf{C}_{rb}$. This minimization is achieved by satisfying the following conditions

$$\frac{\partial \Lambda}{\partial \mathbf{e}_i} = \mathbf{0} \qquad \frac{\partial \Lambda}{\partial \mathbf{C}_{rb_i}} = \mathbf{0} \tag{27}$$

By substituting Equations (26) and (3) into Equation (27) and by performing the differentiation the following expression is obtained

$$\begin{bmatrix} \mathbf{R}_{ei} & \mathbf{R}_{eirb} \\ \mathbf{R}_{eirb}^T & \mathbf{R}_{rb} \end{bmatrix} \begin{Bmatrix} \mathbf{e} \\ \mathbf{C}_{rb} \end{Bmatrix} - \begin{Bmatrix} \mathbf{R}_{s1} \\ \mathbf{R}_{s2} \end{Bmatrix} = \mathbf{0} \tag{28}$$

where $\mathbf{R}_{ei}$ and $\mathbf{R}_{s1}$ are defined in Table 1, and $\mathbf{R}_{eirb}$, $\mathbf{R}_{rb}$, and $\mathbf{R}_{s2}$ are defined in Table 3.

The unknown voltages and rigid body motion coefficients required to achieve the desired shape are determined by solving Equation (28) for $\mathbf{e}$ and $\mathbf{C}_{rb}$. The result is

$$\begin{Bmatrix} \mathbf{e} \\ \mathbf{C}_{rb} \end{Bmatrix} = \begin{bmatrix} \mathbf{R}_{ei} & \mathbf{R}_{eirb} \\ \mathbf{R}_{eirb}^T & \mathbf{R}_{rb} \end{bmatrix}^{-1} \begin{Bmatrix} \mathbf{R}_{s1} \\ \mathbf{R}_{s2} \end{Bmatrix} = \mathbf{0} \tag{29}$$

The magnitudes of C_x and C_y, the coefficients of the translations in the x- and y-directions, are obtained from the difference between the x- and y-coordinates of the points R′ and R, respectively. As in Section 3.2, in these calculations the desired shape is specified in terms of the shape of the reference surface.

3.5 Solution with Nonlinear Strain-Voltage Material Behavior

Equations (12) and (26) apply when the strain-voltage relationship of the piezoelectric material is linear. The analysis could be extended to include piezoelectric materials with nonlinear strain-voltage behavior (Equation (16) in Reference [1]) by minimizing the Λ function with respect to $\mathbf{e}$ (and, if applicable,

Table 3. Definitions of $\mathbf{R}_{eirb}$, $\mathbf{R}_{rb}$ and $\mathbf{R}_{s2}$.

Term	Definition
$\mathbf{R}_{eirb}$	$\bar{\mathbf{w}}^T \iint_\Omega \mathbf{h}^T \left(\mathbf{z}_{rb}^T + \frac{\partial \hat{Z}_{des}}{\partial \hat{x}} \mathbf{x}_{rb}^T + \frac{\partial \hat{Z}_{des}}{\partial \hat{y}} \mathbf{y}_{rb}^T \right) \eta_1 d\hat{x}d\hat{y}$ $+ \bar{\mathbf{u}}^T \iint_\Omega \mathbf{f}^T \left(\mathbf{z}_{rb}^T + \frac{\partial \hat{Z}_{des}}{\partial \hat{x}} \mathbf{x}_{rb}^T + \frac{\partial \hat{Z}_{des}}{\partial \hat{y}} \mathbf{y}_{rb}^T \right) \eta_2 d\hat{x}d\hat{y}$ $+ \bar{\mathbf{v}}^T \iint_\Omega \mathbf{g}^T \left(\mathbf{z}_{rb}^T + \frac{\partial \hat{Z}_{des}}{\partial \hat{x}} \mathbf{x}_{rb}^T + \frac{\partial \hat{Z}_{des}}{\partial \hat{y}} \mathbf{y}_{rb}^T \right) \eta_3 d\hat{x}d\hat{y}$
$\mathbf{R}_{rb}$	$\iint_\Omega \left(\mathbf{z}_{rb} + \frac{\partial \hat{Z}_{des}}{\partial \hat{x}} \mathbf{x}_{rb} + \frac{\partial \hat{Z}_{des}}{\partial \hat{y}} \mathbf{y}_{rb} \right)$ $\left(\mathbf{z}_{rb}^T + \frac{\partial \hat{Z}_{des}}{\partial \hat{x}} \mathbf{x}_{rb}^T + \frac{\partial \hat{Z}_{des}}{\partial \hat{y}} \mathbf{y}_{rb}^T \right) d\hat{x}d\hat{y}$
$\mathbf{R}_{s2}$	$\iint_\Omega \left(\mathbf{z}_{rb} + \frac{\partial \hat{Z}_{des}}{\partial \hat{x}} \mathbf{x}_{rb} + \frac{\partial \hat{Z}_{des}}{\partial \hat{y}} \mathbf{y}_{rb} \right) (\hat{z}_{des} - \hat{z}_o) d\hat{x}d\hat{y}$

with respect to $\mathbf{C}_{rb}$) using a finite-difference quasi-Newton method such as that discussed in Reference [3].

3.6 Numerical Implementation

Solutions to the aforementioned equations must be obtained by numerical means. To generate numerical results, a user-friendly computer code, designated as SHAPE2, was written. The SHAPE2 code uses the numerical integration schemes discussed in Reference [2] to evaluate the integrals appearing in Tables 1 and 3.

4. VERIFICATION

In order to validate the model and the SHAPE2 computer code, results calculated by the code were compared to other analytical, numerical, and experimental results. In these verifications, the initial shape and the desired final shape were entered into the SHAPE2 code. The voltage needed to affect the change in shape was then calculated. The required voltages thus obtained were compared with voltages measured in tests or computed by other analytical means.

The following three problems were included in these comparisons:

1. Cantilever, straight beam made of two continuous piezoelectric layers
2. Flat, rectangular, composite plate with two continuous piezoelectric layers
3. Composite cylindrical shell with one continuous piezoelectric layer

The numerical results generated by the SHAPE1 code were obtained using the material properties listed in Table 5 in Reference [1].

The piezoelectric film behaves in such a way that the relationship between induced strain and applied voltage is linear [4] (see Equation (11) in Reference [1]) and may be characterized by two material constants d_{31} and d_{32}. The values of these properties for KYNAR piezoelectric film are given in Reference [4] and are included in Table 5 in Reference [1].

4.1 Cantilever, Piezoelectric Beam

We consider a 3.15 inch long, 0.394 inch wide and 0.00866 inch thick cantilever beam made of two 0.00433 inch thick KYNAR piezoelectric film layers (Figure 16 in Reference [1]). The top layer is polarized in the direction of an applied voltage and the bottom layer is polarized in the direction opposite an applied voltage. A voltage may be applied across the beam such that the top layer expands while the bottom layer contracts causing a change in shape from an initially straight beam to one whose shape can be described by the equation $z = c \times x^2$. The final shape of the beam is defined by the constant c which depends on the magnitude of the applied voltage and may be calculated from the tip deflection. Lee and Moon [5] reported experimentally measured tip deflections for several different applied voltages. From these data the constant c was obtained and the final shape was determined. This final shape and the originally flat shape were used by SHAPE2 to predict the voltage needed to attain the prescribed shape change. This procedure was repeated at five different voltages, and the resulting predictions of SHAPE2 appear in Figure 8. The voltages predicted by SHAPE2 are in excellent agreement with Lee and Moon's experimentally applied voltages.

4.2 Composite Plate

We consider a 6.0 inch by 4.0 inch T300/976 graphite/epoxy composite plate with a $[+30/-30]_s$ lay-up (Figure 17 in Reference [1]). There is a 0.004 inch thick continuous layer of KYNAR piezoelectric film bonded to the top and bottom surfaces. Each piezoelectric layer is mechanically isotropic but has orthotropic voltage versus strain behavior. The piezoelectric layers' orientations are such that the direction of largest strain is in the y-direction (see Figure 17 in Reference [1]). The top piezoelectric layer is polarized in the direction of an applied voltage and the bottom layer is polarized in the direction opposite an applied voltage. A voltage across both films causes the plate to be in pure bending.

An applied voltage was chosen and the corresponding final shape was calculated by the SHAPE1 code [1]. This final shape and the originally flat shape were used by SHAPE2 to predict the voltage needed to attain the prescribed shape change. This procedure was repeated at four different voltages, and the resulting predictions of SHAPE2 appear in Figure 9. As can be seen, the voltages pre-

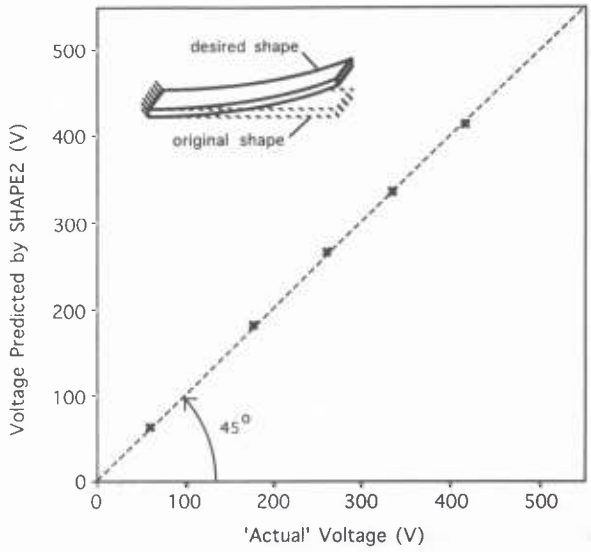

Figure 8. *Comparison of the "actual" and predicted voltages for a cantilever, piezoelectric beam (see Figure 16 in Reference [1] for dimensions).*

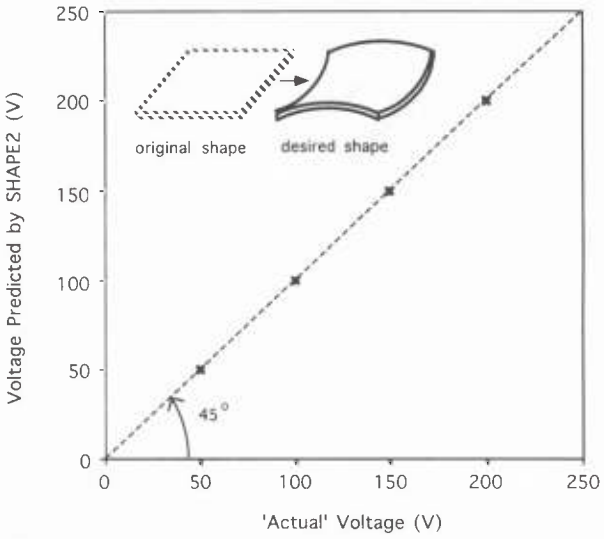

Figure 9. *Comparison of the "actual" and predicted voltages for a composite plate (see Figure 17 in Reference [1] for dimensions). "Actual" is the input voltage to SHAPE1.*

dicted by SHAPE2 are in excellent agreement with the corresponding voltages used as input to SHAPE1.

4.3 Composite Shell

The aforementioned sample problems apply to flat beams and plates. No analytical or experimental results are available for the shape change of curved elements. Tests were therefore performed with a curved element to generate data which can be compared to the results of the model.

A 10.6 inch long and 6.0 inch wide rectangular shell was constructed of six layers of T300/976 unidirectional graphite/epoxy tape (Figure 21 in Reference [1]). The layup was $[90/+60/-60]_s$ with the 0° direction along the longitudinal direction. The radius of the inner surface was 12.0 inches. A continuous layer of KYNAR piezoelectric film [4] was adhesively bonded to the outer radius surface by Loctite DEPEND adhesive. The piezoelectric film is mechanically isotropic but has orthotropic voltage versus strain behavior. The piezoelectric layer's orientation is such that the direction of largest strain is in the lengthwise direction.

One of the corners of the shell was clamped. A voltage was "applied" across the film and the resulting shape change was calculated by the SHAPE1 code. This final shape and the original shape ($z = 0.043 \times y^2$) were used by SHAPE2 to predict the voltage needed to attain the prescribed shape change. This procedure was repeated at five different voltages, and the resulting predictions of SHAPE2 appear in Figure 10. As can be seen, the voltages predicted by SHAPE2 are in excellent agreement with the corresponding voltages used as input to SHAPE1.

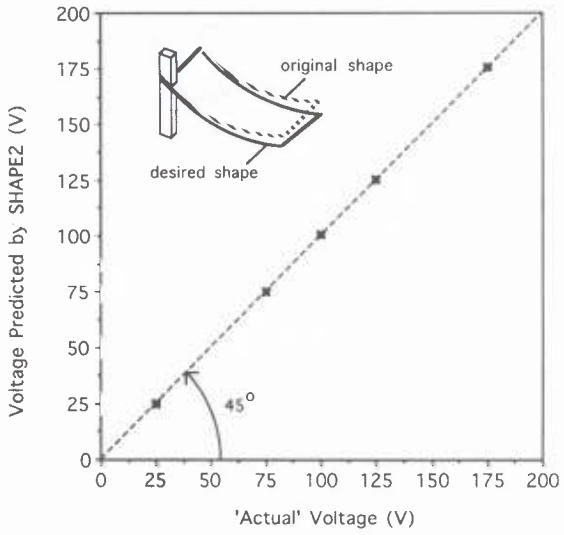

Figure 10. *Comparison of the "actual" and predicted voltages for a composite shell (see Figure 21 in Reference [1] for dimensions). "Actual" is the input voltage to SHAPE1.*

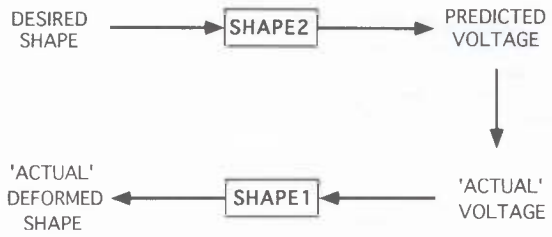

Figure 11. *Flowchart describing how the "actual" deformed shape is calculated.*

The aforementioned comparisons presented for the three problems show that, at least for these problems, the SHAPE2 code can predict the voltages necessary to achieve a desired shape with good accuracy. These results lend confidence to the SHAPE2 code.

5. SAMPLE PROBLEMS

Solutions to sample problems were obtained to illustrate the capability of the SHAPE2 code and the type of results provided by the code. The same five cases were studied as with the SHAPE1 code in [1]:

1. Straight, composite, sandwich beam
2. Curved, composite, sandwich beam
3. Flat, rectangular, composite, sandwich plate
4. Composite, cylindrical, sandwich shell
5. Composite, axisymmetric, sandwich shell

Each of the above structural elements consisted of a 0.10 inch thick aluminum honeycomb core covered on each side by a T300/976 graphite-epoxy face sheet (Figure 23 in Reference [1]). There was a 0.004 inch thick layer of KYNAR piezoelectric film placed on the top and bottom of both face sheets. Thus, the lay-up was $[p/\pm 45/0/p/core/p/0/\mp 45/p]$ with the 0° direction aligned with the x-axis. Each structure was rigidly supported at its midpoint. The material properties used in all calculations are listed in Table 5 in Reference [1].

In each problem, a desired shape was chosen. Next, the SHAPE2 code (with $\Gamma = 1 \times 10^{-15}$ in^2/V^2) was used to predict the voltage which should be applied across each piezoelectric film layer in order to obtain the desired shape. Note that a positive voltage implies that the voltage is applied in the same direction as the polarization of the layer, while a negative voltage implies that the voltage is applied in a direction opposite the polarization of the layer. The "actual" deformed shape (i.e., the shape the element would have if the voltages predicted by SHAPE2 were applied), was calculated by SHAPE1 using—as input—the voltages given by SHAPE2 (Figure 11).

The first two problems considered 8.0 inch long and 1.0 inch wide straight and curved beams. For the curved beam, the reference mid-surface was described by the function $z_o = -0.05 \times x^2$. The third problem was an 8.0 inch long and 6.0 inch wide flat plate, while the fourth problem was an 8.0 inch long and 6.0 inch

Table 4. Equations for the desired shapes of sample problems.

Original Shape	Desired Shape
Straight beam	$-1.2 \times 10^{-5}x^2$
Curved beam	$-5.0012 \times 10^{-2}x^2$
Flat plate	$-1 \times 10^{-5}x^2 + 9 \times 10^{-7}xy - 4 \times 10^{-6}y^2$
Cylindrical shell	$-5.001 \times 10^{-2}x^2 + 8 \times 10^{-7}xy - 3 \times 10^{-8}y^2$
Axisymmetric shell	$-5.0004 \times 10^{-2}x^2 + 1 \times 10^{-7}xy - 4.9997 \times 10^{-2}y^2$

wide cylindrical shell with the reference mid-surface described by the function $z_o = -0.05 \times x^2$. The fifth problem was an axisymmetric cap with reference mid-surface given by $z_o = -0.05 \times (x^2 + y^2)$. The original shapes, desired shapes (Table 4) and "actual" deformed shapes of each of the above five structural elements are given in Figures 12 through 14.

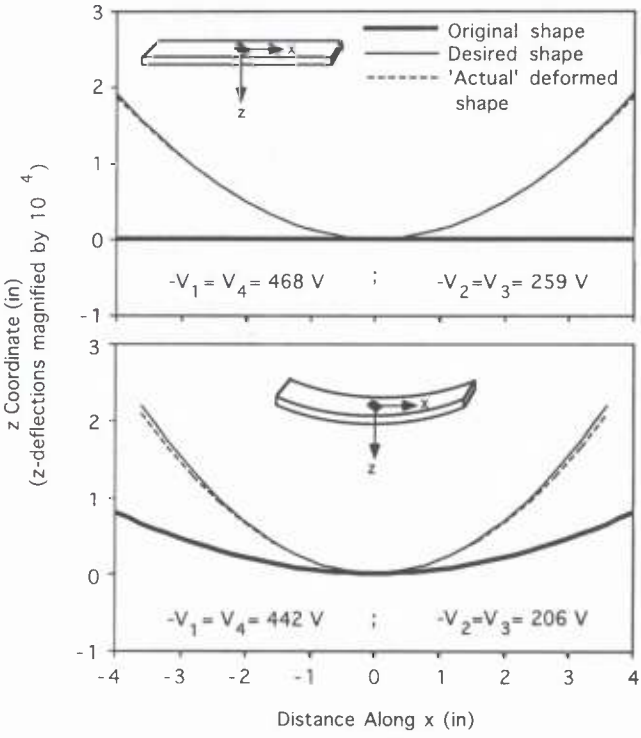

Figure 12. *Predicted voltages and the desired and "actual" deformed shapes for a straight and a curved composite beam. Voltages shown are applied to the actuators indicated in Figure 23 in Reference [1].*

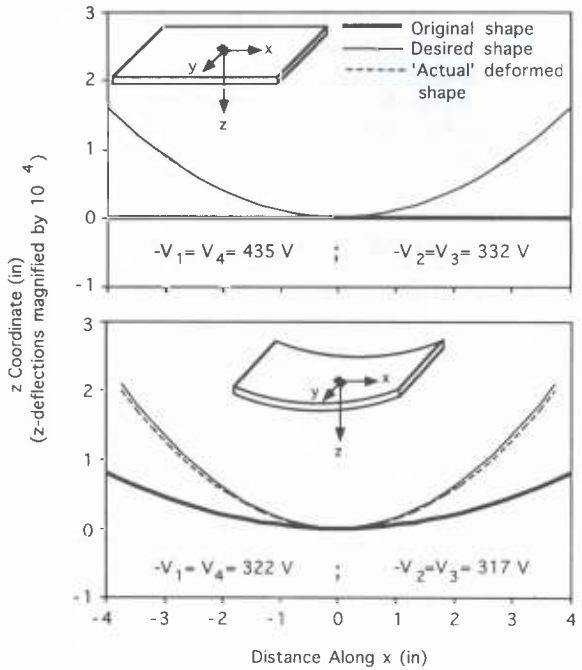

Figure 13. *Predicted voltages and the desired and "actual" deformed shapes for a composite flat plate and a composite cylindrical shell. Voltages shown are applied to the actuators indicated in Figure 28 in Reference [1].*

In the aforementioned problems, it was assumed that the piezoelectric film was continuously covering the entire surface. To illustrate the use of the SHAPE2 code with patches, one sample problem was studied where the desired shape was achieved by the use of piezoelectric patches. In this problem, the deflection of an 7.75 inch long and 1.0 inch wide straight beam was investigated. The cross section of the beam has three layers of T300/976 graphite-epoxy with lay-up [90/0/90] and six 1.0 inch long, 1.0 inch wide and 0.01 inch thick KYNAR piezoelectric patches, as shown in Figure 15. The desired shape was $z = -1 \times 10^{-5}x^4$. The voltages required to achieve the desired shape were calculated by the SHAPE2 code for three values of the weight factor Γ ($\Gamma = 10^{-12}$ in^2/V^2, $\Gamma = 10^{-13}$ in^2/V^2 and $\Gamma = 10^{-14}$ in^2/V^2). For $\Gamma = 10^{-14}$ in^2/V^2, the desired and the "actual" deformed shapes are practically identical as shown in Figure 15. The voltages applied to the actuators are also indicated in the figure. The "actual" shapes calculated by the SHAPE1 code for the other values of Γ are presented in Figure 16 together with the voltages predicted by the SHAPE2 code which would need to be applied to achieve the shapes shown. Note that as Γ increases, the agreement between the "actual" and desired shapes becomes worse. However, it is im-

portant to observe that, coupled with the increase in distance between the two shapes, the amount of voltage which must be applied becomes significantly lower. Hence, if the inaccuracy in shape resulting from a larger value of Γ ($\Gamma = 10^{-12}$ in^2/V^2), is acceptable, then the voltage requirements can be reduced.

The results of the above sample problems illustrate the applicability of the SHAPE2 code to several geometries.

6. CONCLUDING REMARKS

A model was developed which describes the changes in shapes of composite beams, plates and shells containing embedded and surface mounted piezoelectric actuators. The model provides the voltages needed to achieve a specified desired shape. The code can also be used to provide, during actual service, the voltages needed to achieve desired shape changes. Hence, this code, in combination with the code developed in Reference [1], can provide the tools needed to affect real time shape control.

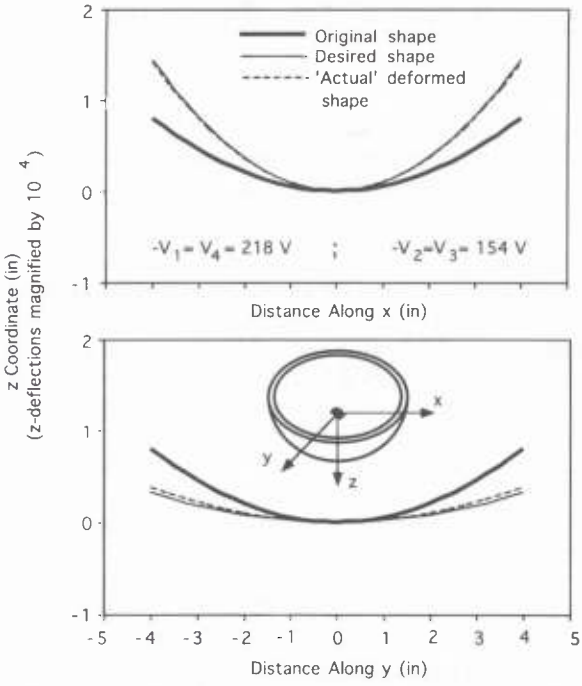

Figure 14. *Predicted voltages and the desired and "actual" deformed shape for an axisymmetric composite shell. Voltages shown are applied to the actuators indicated in Figure 23 in Reference [1].*

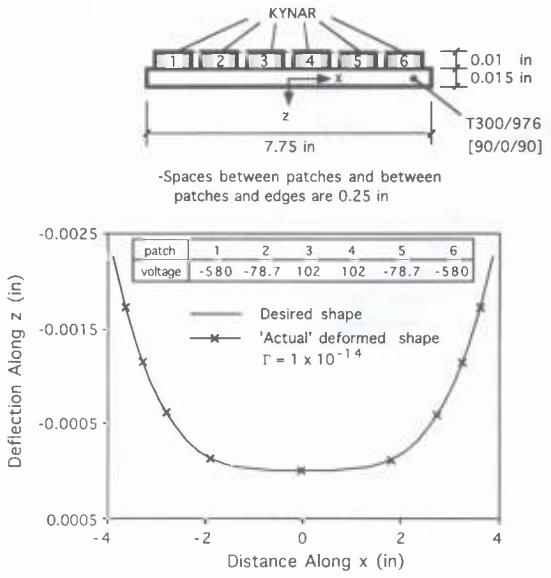

Figure 15. *Voltages predicted by SHAPE2, and the desired and "actual" deformed shape for a composite beam with piezoelectric patches.*

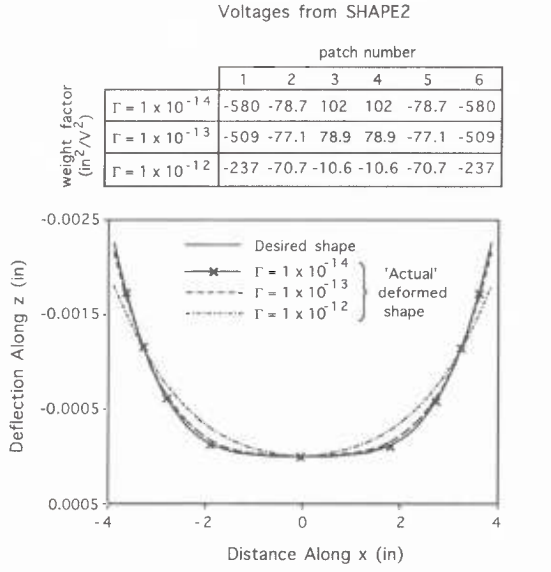

Figure 16. *Voltages predicted by SHAPE2 and the desired and "actual" deformed shape for a composite beam with piezoelectric patches for three values of* Γ *(see Figure 15 for beam dimensions).*

REFERENCES

1. Koconis, D. B., L. Kollár and G. S. Springer. 1994. "Shape Control of Composite Plates and Shells with Embedded Actuators. I. Voltage Specified," *Journal of Composite Materials*, 28(3): 262–285.
2. Koconis, D. B. 1993. "Shape Control of Composite Plates and Shells Using Embedded Actuators," Ph.D. thesis, Stanford University.
3. Gill, P. E., W. Murray and M. H. Wright. 1981. *Practical Optimization*. Academic Press.
4. 1987. "Properties of KYNAR Piezo Film," in *KYNAR Piezo Film Technical Manual*. Valley Forge, PA: ATOCHEM, pp. 9–20.
5. Lee, C. K. 1990. "Theory of Laminated Piezoelectric Plates for the Design of Distributed Sensors/Actuators. Part I: Governing Equations and Reciprocal Relationships," *Journal of the Acoustic Society of America*, 87:1144–1158.